12-15-2000

Electrons in image states near roughened metal surfaces

Brian K. Clark
Illinois State University

Brian W. Gregory
Illinois State University

Jean M. Standard
Illinois State University

Electrons in image states near roughened metal surfaces

B. K. Clark*
Department of Physics, Illinois State University, Normal, Illinois 61790-4560

B. W. Gregory† and J. M. Standard‡
Department of Chemistry, Illinois State University, Normal, Illinois 61790-4160

(Received 29 June 2000)

Electrons near roughened Ag and Au surfaces with chemisorbed dielectric overlayers of alkanethiol or alkaneselenol self-assembled monolayers are shown to move within the sulfur or selenium head-group layer on the metal terraces. The electrons exist in image states with respect to Ag or Au step edges. There is no substantial image force between the electrons and the terraces.

I. INTRODUCTION

The attractive force between a metal surface and a nearby electron can be described by the classical method of images and leads to a $1/z$ potential, where z is the distance between the electron and metal surface. As the electron approaches the metal surface, it has some probability of penetrating the surface, and the potential can be described by the nearly free-electron (NFE) model. There is excellent agreement between experimentally measured image state energies and theoretical calculations for palladium and the coinage metals[1–4] when this model is applied to the interaction of electrons with clean and smooth metal surfaces. Bound image state energies described by a Rydberg series are observed for these surfaces. The degree of electron penetration into the metal is determined by the location of the image state binding energy with respect to the band structure of the bulk metal. The wave function for an energy level that coincides with a band gap attenuates in the bulk metal, so the wave function appears as a surface state with hydrogenic character external to the metal. An electron with an energy level coincident with the either a valence or a conduction band propagates into the metal, and its wave function appears as a surface resonance.

Experiments with various overlayers physisorbed onto smooth metal surfaces show image state or quantum well-like energies. Dielectric overlayers physisorbed onto metal surfaces, such as various alkanes on silver,[5–7] yield image state energies that decrease by as much as a factor of 2 from the clean metal case as the dielectric overlayer thickness is increased. Alternatively, when a sufficiently thick xenon overlayer is placed on silver, a conduction band forms within the overlayer, and the electron exists in a range of quantum well states.[8–10]

Image states associated with roughened metal surfaces have been observed for chemisorbed self-assembled monolayers (SAM's) of alkanethiols and alkaneselenols on roughened gold and silver surfaces with a resolution of approximately 0.1 meV via surface enhanced Raman scattering (SERS).[11] Consequently, these systems provide an opportunity to explore the character of image states in the presence of roughened surfaces and chemisorbed dielectric overlayers. A sketch of a portion of an alkanethiol coated roughened gold substrate is shown in Fig. 1. The use of SERS has permitted the observation of spectra produced from scattering between eight states whose binding energies range from -0.155 eV to -0.006 eV relative to the vacuum energy. Since the Raman spectra obtained via SERS involve electronic transitions between image state energy levels, the process is referred to as SEERS,[11] where the second E signifies the electronic nature of the scattering. Image states associated with smooth surfaces are usually probed using two-photon photoelectron emission spectroscopy (2PPE) with a typical resolution of 50 meV.[4] Because of its limited resolution, 2PPE cannot be expected to resolve states with binding energies as small as those observed in the SEERS experiments.

We begin with a brief discussion of the major experimental results for roughened metal surfaces. Next, we present the computer model that allows the effects of surface roughness and dielectric overlayer on allowed image state levels to be explored. Finally we discuss the results of computer simulations for the model roughened system.

II. ROUGHENED METAL SURFACES

Virtually identical alkanethiol SEERS spectra are obtained for roughened Ag and Au electrodes,[11,12] aggregated Au colloidal monolayer films,[12] or aggregated Au colloid.[13] Unlike surfaces cleaved to yield specific terrace and step edge orientations, roughened surfaces have an irregular distribution of edges and terraces. The effective system resolution in these experiments is measured to be 1.2 cm^{-1} (0.15

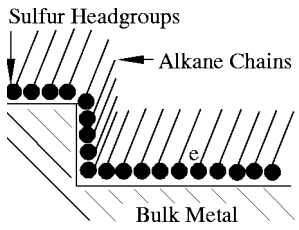

FIG. 1. Sketch of alkanethiol coated roughened gold substrate. The electron in an image state is denoted with the letter *e*. The correct placement and direction of motion of the electron is discussed in Sec. III.

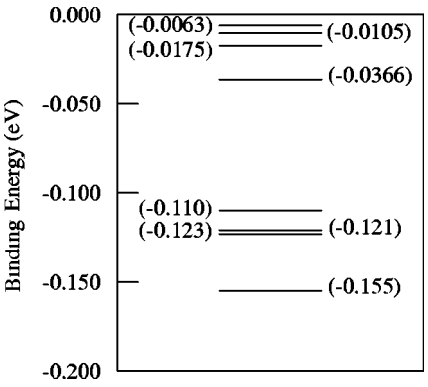

FIG. 2. Image state energy level diagram.

meV), and the actual measured linewidths are between 4 and 9 cm^{-1} (0.5 and 1.1 meV). An energy-level diagram derived from a SEERS spectrum obtained by laser irradiation of a $CH_3(CH_2)_9SH$ SAM on a roughened gold substrate is displayed in Fig. 2.[11] With the exception of intensity, spectra are identical (within the limit of resolution) for $R(CH_2)_mSH$ SAM's ($R=CH_3HC$, or HOOC) whose alkyl chain lengths extend from $m=8$ to 17 for ^{32}S, ^{34}S, or Se headgroups, and for perdeuterated alkyl chains. There is also no observable change when spectra are recorded with the films in air or aqueous solution. The most intense spectra occur for $m \geqslant 9$ and become less intense as the chain length is decreased to $m=7$. No spectra are observed for shorter chain lengths at room temperature. The resulting dielectric thickness ranges from ~6 Å for a 6 carbon chain to ~20 Å for an 18 carbon chain. The independence of the SEERS spectra and the associated image state energy level spacings with respect to the variations discussed above strongly suggests that the electron is constrained to remain within the dielectric layer.

Quantum-mechanical calculations[2] predict that the energy levels of an electron located near a metal surface are at energies E_n, where

$$E_n = -\frac{0.85\ \text{eV}}{(n+\delta)^2}. \tag{1}$$

Here, n is the traditional principal quantum number and δ is the quantum defect due to screening. The constant value of 0.85 eV (13.6 eV/16) indicates that E_n is reduced by a factor of 16 from the hydrogen atom case because the electron at a distance z from the metal surface is separated from its image charge by $2z$.[14] A further reduction in the image state binding energy is expected for a metal surface covered with a semi-infinite dielectric film, the magnitude of which is proportional to $1/\epsilon^2$, where ϵ is the dielectric constant of the film.

The lowest four energy levels observed in the SEERS spectra are collectively attributed to the $n=1$ image state. A fit of the four highest observed energy levels and the energy level at -0.121 eV to Eq. (1) yields $\delta=0.23$. This simple fit assumes an infinite dielectric, and the effects of the real metal substrate are hidden in the parameter δ. A further limitation of the simple theory is that it does not allow for multiple $n=1$ energy levels. One possible explanation for the four observed $n=1$ levels is that the electrons interact with different crystal faces of the metal substrate. However, if this is the case, the apparent coincidence of the higher n levels must be explained.

III. COMPUTER MODEL

The model potential applied to an electron interacting with a metal substrate is obtained by joining the potential inside the bulk metal determined using NFE theory[15] with the potential external to the metal derived from the classical theory of images. This type of potential has been successfully employed to model the electron interaction with clean metal surfaces[1–4,16–19] and surfaces with dielectric overlayers.[5–7,9,10] It has also been successfully applied to metal overlayers on metal substrates.[20–22] The potential in the bulk metal is given by

$$U(z) = -V_0 + 2V_G\cos(Gz), \quad z < z_0, \tag{2}$$

where one-half the band gap is represented by V_G, where $G=2\pi/a$ is the reciprocal lattice vector, and a is the lattice spacing. The same notation as that of Lenac, Sunjic, Conrad, and Kordesch (LSCK) is employed.[1] The parameter $V_0 = E_G - V_G + \Phi_0 - E_L$, where

$$E_G = \frac{\hbar^2(G/2)^2}{2m} \tag{3}$$

places the mean energy of the potential with respect to the center of the band gap, where Φ_0 is the work function, and E_L is the energy at the lower edge of the band gap. Both Φ_0 and E_L are measured with respect to the Fermi level. The potential outside the metal is modeled as a constant potential,

$$U(z) = -U_0, \quad 0 < z_0 \leqslant z < z_i^*, \tag{4}$$

and image potential,

$$U(z) = -\frac{e^2}{16\pi\epsilon\epsilon_0(z-z_i)}, \quad z \geqslant z_i^*. \tag{5}$$

The value of z_0 is the location at which $U(z)$ in Eq. (2) equals $-U_0$. The location of the image plane is at $z_i \leqslant z_i^*$. The value of $U(z)$ in Eq. (5) equals the constant potential $-U_0$ at z_i^*. The permittivity of free space is ϵ_0. One-dimensional potentials for a clean Ag(100) surface and a surface with a dielectric overlayer ($\epsilon=2.33$) of semi-infinite extent, are shown in Fig. 3 as traces (a) and (b), respectively. Energy levels for the image state system are determined by numerically solving the time-independent Schrödinger equation for the potential given by Eqs. (2), (4), and (5) using the Cooley-Cashion-Zare method.[23–25] The numerical solution does not require the use of an effective mass in the Schrödinger equation as it does when the eigenfunctions in the bulk metal are assumed to be in the form of Bloch waves. Instead, V_0 (or equivalently, E_G) is varied slightly to achieve agreement with experimental observation. Rows a and b in Table I show the agreement between the three lowest image state energies for clean Pd(111) calculated in this paper and the results of LSCK for $U_0=5.5$ eV and $z_i=2.1$ Å. Experimental measurements of the two lowest image state energies for clean Pd(111) are presented in row c. Image state energies calculated in this paper for clean Pd(111) are shown in

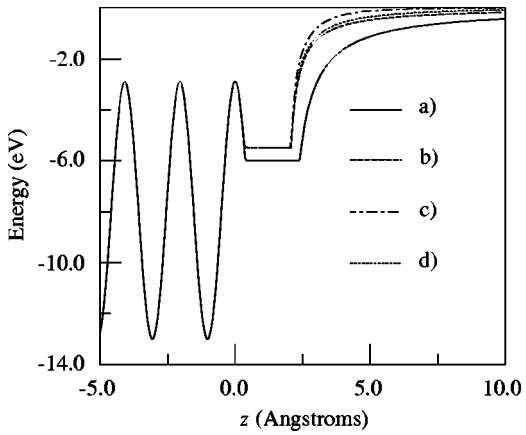

FIG. 3. Potential-energy curves for an electron interacting with a) a single clean Ag(100) surface, (b) the same surface with a dielectric overlayer ($\epsilon=2.33$), (c) two intersecting Ag(100) surfaces where the electron is at distance of 3 Å from surface *ZY* (Fig. 4) for $\epsilon=2.33$, and (d) two intersecting Ag(100) surfaces in the same arrangement as (c) but where the electron is at distance of 12 Å from surface *ZY*. The dielectric overlayers fill all space outside the Au.

row d for the same parameters as row b, except $z_i=1.7$ Å. The Pd results show that the calculated energies are very sensitive to the image plane location.

Rows e through h in Table I present a comparison of the calculated values for clean Ag(100) and Au(100) surfaces with the available experimental values for the $n=1$, 2, and 3 energy levels. The parameters V_0, U_0, and z_i do not represent best fit values, but rather are determined by manually

TABLE I. Energies (eV) of the $n=1$, 2, and 3 image states on clean metal surfaces calculated in this paper. Theoretical and experimental values from the literature are included for Pd(111) and experimental values from the literature are included for Ag(100) and Au(100) for comparison.

	$n=1$	$n=2$	$n=3$
Pd(111)[a]	−0.72	−0.22	−0.096
Pd(111)[b]	−0.699	−0.209	−0.0947
Pd(111)[c]	−0.55	−0.15	
Pd(111)[d]	−0.546	−0.176	−0.0862
Ag(100)[e]	−0.529	−0.172	−0.0825
Ag(100)[f]	−0.533	−0.162	−0.075
Au(100)[g]	−0.55	−0.18	−0.08
Au(100)[h]	−0.63		

[a]Reference 1.
[b]This work $V_0=8.78$ eV, $U_0=5.50$ eV, $z_i=2.10$ Å. $G=2.80$ Å^{-1}, $V_G=3.3$ eV, and $\Phi_0=5.6$ eV from Ref. 1.
[c]Reference 22, only $n=1$ and 2 are reported.
[d]This work $V_0=8.78$ eV, $U_0=5.50$ eV, $z_i=1.70$ Å, $G=2.80$ Å^{-1}, $V_G=3.3$ eV, and $\Phi_0=5.6$ eV from Ref. 1.
[e]This work, $V_0=7.95$ eV, $U_0=6.00$ eV, $z_i=1.80$ Å, $G=3.075$ Å^{-1}, $V_G=2.53$ eV, and $\Phi_0=4.43$ eV from Ref. 26.
[f]Reference 3.
[g]This work, $V_0=10.22$ eV, $U_0=6.00$ eV, $z_i=1.50$ Å, $G=3.082$ Å^{-1}, $V_G=2.15$ eV, and $\Phi_0=5.47$ eV from Ref. 27.
[h]Reference 28, only $n=1$ is reported.

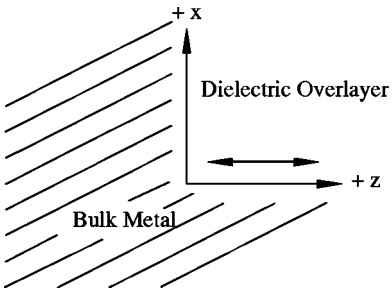

FIG. 4. Schematic of model system used for calculations as described in the text. The region defined by x, $z>0$ is vacuum for clean metal surfaces or filled with a dielectric for surfaces with overlayers. The electron is constrained to move in the direction of the double-ended arrow.

adjusting each parameter to generate energy-level spacings and values that are representative of the experimental data. The values of V_0 for the (100) surfaces are in good agreement with the values determined from the corresponding band parameters.

Since the experimental SEERS measurements are carried out on a roughened surface, the electron is generally near at least two crystal faces of the metal. To determine the effect of the presence of a second surface on the image state spectra, the energies of a model system consisting of two orthogonal metal surfaces is examined, as shown in Fig. 4. One surface is in the *xy* plane (surface *XY*), and extends over all *y* space and from $x=0$ to $x=\infty$. The second surface is in the *zy* plane (surface *ZY*), and extends over all *y* space and from $z=0$ to $z=\infty$. All space for $x\leqslant 0$ or $z\leqslant 0$ is metal. The space for $x>0$ and $z>0$ is treated as either vacuum ($\epsilon=1$) or dielectric ($\epsilon>1$). The image potential in this region is

$$U(x,z)=-U_0, \tag{6}$$

$$0<z_0\leqslant z<z_i^* \quad \text{or} \quad 0<x_0\leqslant x<x_i^*,$$

and

$$U(x,z)=-\frac{e^2}{16\pi\epsilon\epsilon_0}\left\{\frac{1}{z_d}+\frac{1}{x_d}-\frac{1}{(z_d^2+x_d^2)^{1/2}}\right\}, \tag{7}$$

$$z_d=z-z_i, \quad x_d=x-x_i,$$

$$z\geqslant z_i^* \quad \text{and} \quad x\geqslant x_i^*.$$

The variables x_0, x_i, and x_i^* fulfill the equivalent roles for the second surface as the *z* variables do for the single surface.

The Schrödinger equation for an electron interacting with two intersecting planes is not separable into two independent equations for the two perpendicular directions of motion. Since experimental evidence shows that the energy levels are independent of monolayer thickness and external environment, the electron is constrained to move in the dielectric at a fixed distance from and parallel to one surface (surface *ZY*) in this model. When solving the Schrödinger equation for an electron constrained to move parallel to the *ZY* plane at a fixed distance *x*, the $1/x$ term in the potential is ignored. By ignoring this constant term, potentials for all constant values of *x* converge to the same vacuum level at large *z*. The potential inside the bulk metal is still given by Eq. (2), for an

TABLE II. Energies (eV) of the $n=1-5$ image states calculated in this paper for Ag(100) and Au(100). The last row is comprised of experimental values for Au from Fig. 2.

$n=1$	$n=2$	$n=3$	$n=4$	$n=5$
		Ag(100)		
−0.529[a]	−0.172	−0.0825	−0.0481	−0.0314
−0.283[b]				
−0.122[c]	−0.0346	−0.0160	−0.0092	−0.0060
−0.0248[d]				
		Au(100)		
−0.129[e]	−0.0358	−0.0164	−0.0094	−0.0060
		Exp.[f]		
−0.121	−0.0366	−0.0175	−0.0105	−0.0063

[a]Single surface: $\epsilon=1$, $V_0=7.95$ eV, $U_0=6.00$ eV, $z_i=1.80$ Å.
[b]Two surface: $\epsilon=1$, $V_0=7.95$ eV, $U_0=6.00$ eV, $z_i=1.80$ Å, electron is 12 Å from surface *ZY*.
[c]Single surface: $\epsilon=2.33$, $V_0=7.95$ eV, $U_0=5.50$ eV, $z_i=1.80$ Å.
[d]Two surface: $\epsilon=2.33$, $V_0=7.95$ eV, $U_0=5.50$ eV, $z_i=1.80$ Å, electron is 12 Å from surface *ZY*.
[e]Single surface: $\epsilon=2.33$, $V_0=10.00$ eV, $U_0=6.00$ eV, $z_i=1.50$ Å.
[f]Reference 11.

electron constrained to move parallel to the z axis. Sample potentials for an electron constrained at distances of 3 and 12 Å from surface *ZY* are shown in Fig. 3 for $\epsilon=2.33$ as traces (c) and (d), respectively. Calculated energy levels, obtained from solving the Schrödinger equation for the resulting image state potential combined with the bulk potential for Ag(100), are shown in Table II. While calculations were performed for electron distances of 3, 6, and 12 Å from surface *ZY*, only for the electron 12 Å from surface *ZY* is there a bound energy level in the image state energy regime. Surface states with binding energies greater than 1 eV are ignored in this paper, because there are no experimental results for the roughened surfaces with which to compare.

Whenever the electron is near two surfaces, the potential rises sharply, much like a simple step potential as illustrated in Fig. 3, and the energy levels are pushed toward the vacuum energy level. At large z, the potential converges to the vacuum level much more quickly in the presence of two surfaces than for one surface. The energy levels are also more weakly bound for the $\epsilon=2.33$ case than for the $\epsilon=1$ case. Our results show that energy levels calculated for an electron near two intersecting orthogonal surfaces do not agree with experimentally determined energy levels, regardless of the value of ϵ. Increasing the intersection angle by 10° to 20° is not expected to add more than one additional bound energy level.

While the calculations for two orthogonal intersecting surfaces are not in agreement with the experimental data, the calculated energy levels for an electron interacting with a single surface for $\epsilon=2.33$ (Table II) are in good agreement with the experimental results from Fig. 2. The similarity of the calculated Ag(100) and Au(100) binding energies demonstrates how the SEERS spectra for image state electrons can be identical to within experimental resolution for the two different metals. The dielectric constant is selected to be $\epsilon=2.33$ because this fits the experimental results for the Ag(100) surface as outlined in Table II. Dielectric constants that differed by more than 0.2 from 2.33 give energy levels that are not representative of the experimentally measured energy levels. The values of the parameters V_0, U_0, and z_i are varied in a similar manner as for clean metals. The image plane location is generally treated as a constant value for each crystal surface. However, there is expected to be a variation in the image plane position with image state quantum number because of the variation of electron dynamics between levels.[18] The image plane shift will then be greatest between the $n=1$ and 2 energy levels. More detailed modeling of the image plane position may reduce the discrepancy between the calculated $n=1$ energy levels for Au(100) and Ag(100).

This paper shows that the energy levels presented in Fig. 2 result from electrons interacting with single surfaces and constrained to stay within dielectric overlayers. This is most easily visualized if we identify surface *ZY* as a terrace to which alkanethiols (or alkaneselenols) have bonded. Surface *XY* similarly corresponds to a step edge. Based on the calculated electron probability distributions and energy levels, an electron must be able to move on the order of 10 nm from a step edge without contacting an opposing step edge to produce the experimental energy-level spacing. If opposing step edges are closer together, the $1/z$ potentials from each step edge converge in the middle, and electron probability functions and energy levels that are characteristic of quantum wells arise. Quantum well energy spacings are not consistent with the experimental observations. Since the calculations show that the SEERS results come from a system in which the electron experiences an image force with respect to only one surface, there must not be an image force with respect to the terrace surface. Other work[5–7] clearly shows that electrons do experience image forces with metal surfaces having physisorbed alkane overlayers. In the chemisorbed systems modeled in this work, the image force is only eliminated if the electron is in the vicinity of the terrace image plane, which is about 2 Å above the terrace. This is also the approximate location of the sulfur (selenium) layer adjacent to the metal surface. Therefore, the electron depicted in Fig. 1 must be constrained to move in a plane located above the terrace in the region that coincides with the sulfur (selenium) layer. The bond between the alkanethiol (alkaneselenol) headgroup and metal surface must play a significant role in constraining the motion of the electron perpendicular to the terraces.

IV. CONCLUSION

The results presented here show that the observed SEERS spectra of roughened Ag and Au surfaces with chemisorbed alkanethiol (alkaneselenol) overlayers are produced by electrons constrained to move within the sulfur (selenium) layers on the terraces. These electrons form image states with Ag or Au step edges. There is no substantial image force between the electrons and the terraces. Finally, the origin of the four $n=1$ energy levels remains ambiguous, but most likely reflects image state electrons interacting with the (100), (111), and two other crystallographic surfaces. Further work must also identify the source of image state electrons.

*Corresponding author: Email: bkc@entropy.phy.ilstu.edu
†Email: bgrego@ilstu.edu
‡Email: standard@ilstu.edu

[1] Z. Lenac, M. Sunjic, H. Conrad, and M. E. Kordesch, Phys. Rev. B **36**, 9500 (1987).
[2] T. Fauster, Appl. Phys. A: Solids Surf. **59**, 479 (1994).
[3] W. Steinmann, Phys. Status Solidi B **192**, 339 (1995).
[4] T. Fauster and W. Steinmann, *Photonic Probes of Surfaces* (Elsevier, New York, 1995).
[5] J. R. L. Lingle, N. H. Ge, R. E. Jordan, J. D. McNeill, and C. B. Harris, Chem. Phys. **205**, 191 (1996).
[6] J. R. L. Lingle, N. H. Ge, R. E. Jordan, J. D. McNeill, and C. B. Harris, Chem. Phys. **208**, 297 (1996).
[7] C. B. Harris, N. H. Ge, J. R. L. Lingle, J. D. McNeill, and C. M. Wong, Annu. Rev. Phys. Chem. **48**, 711 (1996).
[8] W. R. Merry, R. E. Jordan, D. F. Padowitz, and C. B. Harris, Surf. Sci. **295**, 393 (1993).
[9] J. D. McNeill, J. R. L. Lingle, R. E. Jordan, D. F. Padowitz, and C. B. Harris, J. Chem. Phys. **105**, 3883 (1996).
[10] C. M. Wong, J. D. McNeill, K. J. Gaffney, N. H. Ge, A. D. Miller, J. S. H. Liu, and C. B. Harris, J. Phys. Chem. B **103**, 282 (1999).
[11] B. K. Clark, B. W. Gregory, A. Avila, T. M. Cotton, and J. M. Standard, J. Phys. Chem. B **103**, 8201 (1999).
[12] G. Chumanov, K. Sokolov, B. W. Gregory, and T. M. Cotton, J. Phys. Chem. **99**, 9466 (1995).
[13] B. W. Gregory (unpublished observations).
[14] W. K. H. Panofsky and M. Phillips, *Classical Electricity and Magnetism* (Addison Wesley, Reading, MA, 1962).
[15] M. C. Desjonqueres and D. Spanjaard, *Concepts in Surface Physics* (Springer, Heidelberg, 1998).
[16] T. Fauster, Appl. Phys. A: Solids Surf. **59**, 639 (1994).
[17] N. V. Smith, Phys. Rev. B **32**, 3549 (1985).
[18] N. V. Smith, C. T. Chen, and M. Weinert, Phys. Rev. B **40**, 7565 (1989).
[19] M. Weinert, S. L. Hulbert, and P. D. Johnson, Phys. Rev. Lett. **55**, 2055 (1985).
[20] N. V. Smith, N. B. Brookes, Y. Chang, and P. D. Johnson, Phys. Rev. B **49**, 332 (1994).
[21] J. E. Ortega, F. J. Himpsel, G. J. Mankey, and R. F. Willis, Phys. Rev. B **47**, 1540 (1993).
[22] R. Fischer, S. Schuppler, N. Fischer, T. Fauster, and W. Steinmann, Phys. Rev. Lett. **70**, 654 (1993).
[23] J. W. Cooley, Math. Comput. **15**, 363 (1961).
[24] J. Tellinghuisen, Comp. Ser. **66**, 51 (1989).
[25] J. K. Cashion, J. Chem. Phys. **39**, 1872 (1963).
[26] S. Schuppler, R. Fischer, N. Fischer, T. Fauster, and W. Steinmann, Appl. Phys. A: Solids Surf. **51**, 322 (1990).
[27] N. E. Christensen and B. O. Seraphin, Phys. Rev. B **4**, 3321 (1971).
[28] D. Straub and F. J. Himpsel, Phys. Rev. B **33**, 2256 (1986).